Development of Natural Gas Injection System for Large-bore Engine

Binbin Sun, Bo Li, Wentao Li, Wenqing Ge and Hongyuan Wei

***Abstract*—Large-bore engines with continuous gaseous fuel supply system generally suffer from low fuel efficiency and instability performance. In order to achieve a more economical and stable engine performance, a multi-point injection system with optimized injection time for natural gas engine was developed in this work. First of all, a fuel injection device with discoid outlet structure was developed. Pseudo linear system was established to achieve proper response speed and seating velocity. After that, a collaborative optimization platform was established using the genetic algorithm and the thermodynamic model, and then an optimal injection strategy was obtained. Finally, the fuel efficiency, stability and power of a high-power gaseous fuel engine were tested. Results showed that compared with the engine with continuous gas supply system, the fuel efficiency of the engine developed in this work was improved by 6.4% under the full load and by 5.7% under the rated speed of 1000r/min. The volatility of exhaust temperature in twelve cylinders was reduced by 37.47% under the rated working condition. The start-up time was reduced by 21.3% and the torque under full load condition was increased by 4.7%.**

***Index Terms*—High-power gaseous fuel engine, multi-point injection system, optimization of injection time, engine efficiency, volatility of exhaust temperature**

I. Introduction

Gaseous fuel supply system has a significant influence on the fuel efficiency and stability of an engine [1]. The electronically controlled fuel supply system is gradually replacing continuous fuel supply system owe to its capacity of achieving multi-point and intermittent fuel injection, which is beneficial to enhancing engine performance [2,3]. However, for large-bore engines developed for special use, such as power plant in mine, continuous gas supply system is still commonly used. It actually leads to inefficient fuel efficiency and serious volatility of cylinder performance [4].

Currently, the development of electronically controlled fuel supply system for high-power engine is still limited. This is due to that the large cyclic fuel supply technology used in high-power engine is different from the vehicle engine where cyclic fuel is small and injection device is designed with globe or needle valve structure [5]. To achieve large-flow injection, a new-type natural gas injection device using moving coil as linear actuator and valve structure as outlet has been proposed [6], and its flow characteristic of the injection device has been studied and optimized [7]. However, further research on the improvement of control performance has rarely been reported.

Injection time is the key parameter index of electronically controlled fuel supply system, which has a great impact on vehicle performance. A great amount of researches on engine injection time optimization have been carried out, and vehicle engine performance has been improved significantly [8,9]. However, there are few reports on injection time optimization for large-bore engine with multi-point natural gas injection system.

Given the above analyses, to improve ideal performance of a high-power gaseous fuel engine, a multi-point fuel supply system was developed. Firstly, the hardware and control strategy of the large-flow injection device were developed and verified. Then, to confirm the optimal injection strategy, an optimization platform based on thermodynamic model of engine and genetic algorithm (GA) was developed. Finally, the fuel efficiency and stability of the high-power gaseous fuel engine were verified.

II. Development of Large-flow Injection Device

Fig. 1 shows the natural gas injector. To achieve the large cyclic supply of natural gas for the large-bore engine, the outlet valve structure was designed. The electronically controlled actuator was basically a coil driven by electromagnetic force. Around the coil, air-gap magnetic field was generated by the permanent magnets in Halbach array. By controlling the magnitude and direction of the current in the coil, Lorentz force was obtained to control the injection time. A displacement sensor was used to provide the feedback signal of the valve position for the controller.

As shown in fig. 2, the controller consists of DSP, power-driven and signal-feedback modules. The DSP is responsible for signal acquisition, control algorithm operation and signal output. TMS320F2812, the signal processor, was used as the central processing unit. Based on the high operational frequency of 150MHz and the floating point of 32 digits, fast response of the actuator was achieved.

Manuscript received July 3, 2020; revised November 3, 2020. This work was supported in part by the National Natural Science Foundation of China under Grant 51875326 and 51805301, the Natural Science Foundation of Shandong under Grant ZR2019BEE043 and ZR2019MEE049, the Postdoctoral Science Foundation of China under Grant 2020M680091, the Postdoctoral Project and QingChuang Technology Project of Shandong under Grant 202003042 and 2019KJB027.

Binbin Sun, is a professor of School of Transportation and Vehicle Engineering, Shandong University of Technology, Zibo, China (e-mail: sunbin_sdut@126.com).

Bo Li, the corresponding author, is a professor of School of Transportation and Vehicle Engineering, Shandong University of Technology, Zibo, China (e-mail: sdutlibo@126.com).

Wentao Li, is with School of Transportation and Vehicle Engineering, Shandong University of Technology, Zibo, China (e-mail: liwentao1213@126.com).

Wenqing Ge, is a professor of School of Transportation and Vehicle Engineering, Shandong University of Technology, Zibo, China (e-mail: gwq@sdut.edu.cn).

Hongyuan Wei, is with School of Transportation and Vehicle Engineering, Shandong University of Technology, Zibo, China (e-mail: 1315503721@qq.com).

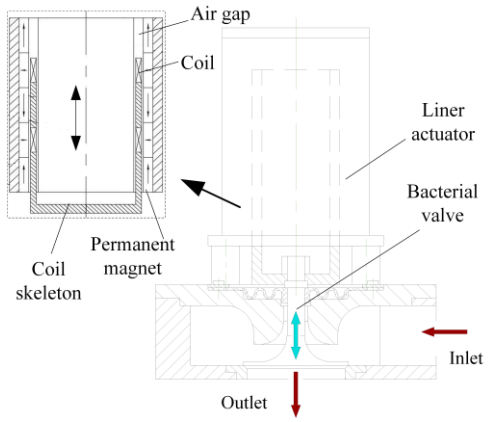

Fig. 1. Structure of the injection device

The power driven module which is responsible for the control of the injection device consists of isolated driving circuit and H-type bridge circuit. The signal feedback module and current sensor were designed to provide current and displacement feedback signals for DSP.

As shown in fig. 3, a control strategy based on the inverse system control method was developed. First of all, according to the physical characteristics of injection device, the nonlinear system equations were derived.

$$\begin{cases} \dot{I} = -\frac{R}{L} I - \frac{k_1}{L} v + \frac{u}{L} \\ \dot{v} = \frac{k_1}{m} I - \frac{c}{m} v \\ \dot{S} = v \end{cases} \tag{1}$$

Where I is the current in the coil, u is the voltage applied to the injection device, S and v represent the speed and displacement of the coil, respectively; m refers to the mass of the moving components, L is the inductance of the coil, k_1 is the back electromotive force constant, and R is the resistance of the coil.

To create a linear control strategy, the inverse system of the device was derived according to the system equations.

$$u = \frac{mL}{k_1} \ddot{y} + \frac{cL}{k_1} \ddot{y} + k_1 \dot{y} + xR \tag{2}$$

Where x is the state vector, $x=[I\ V\ S]^T$, y is the output variable.

Based on the inverse system control theory and the nonlinear system equations, the pseudo linear system was established. The closed-loop transfer function of the system was derived as follow.

$$\frac{Y(s)}{R(s)} = \frac{1}{s^3 + k_2 s^2 + k_3 s_1 + k_4} \tag{3}$$

Where k_2, k_3 and k_4 represent state feedback gains of the system.

State observer and state feedback controller were designed to improve the performance of the device. As the variables used in the state feedback control method were measurable, only the displacement and control current were detected and fed back.

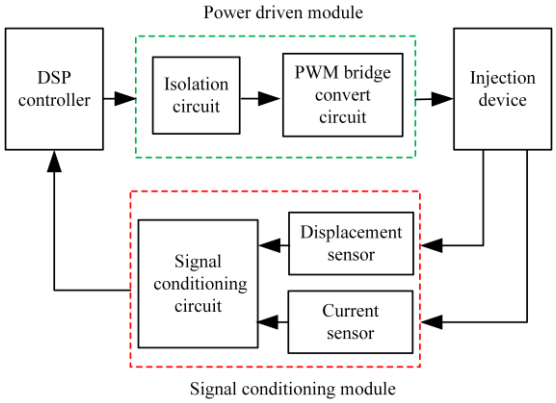

Fig. 2. Hardware schematic diagram of the controller

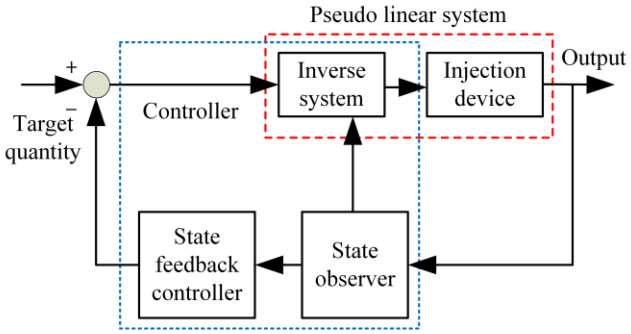

Fig. 3. Controller structure based on inverse system

As shown in fig. 4 (a), during the valve closing process, large current was required to accelerate the valve velocity in the first stage. To avoid hard valve land, a step current was used to decelerate the valve velocity in the second stage. As shown in fig. 4(b), the valve closing process was completed within 5ms and the seating velocity was about 3mm/s. Both high response speed and low seating velocity were achieved. Furthermore, the currents were set to relatively smaller so as to keep the valve widely open and closed, which was conducive to reducing energy consumption.

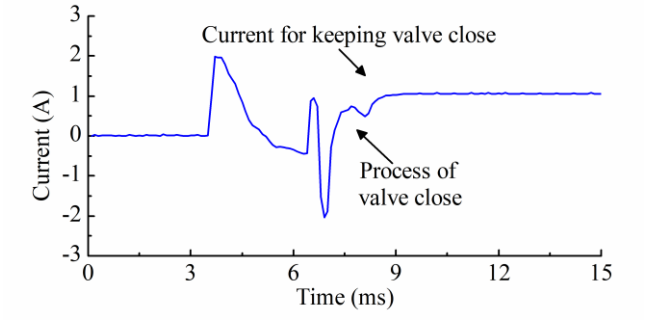

(a) Variation of current

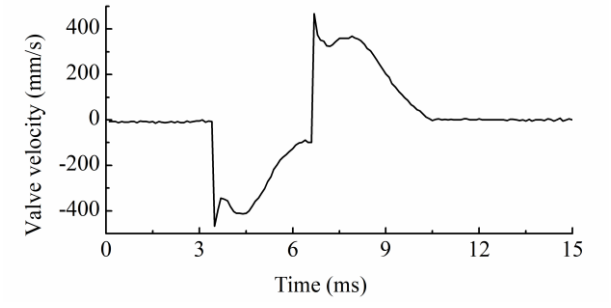

(b) Variation of velocity

Fig. 4. Tested characteristics of the injection device

III. Development of Injection Strategy

A. Development of thermodynamic model

To develop an injection strategy for enhancing the optimal fuel efficiency, the thermodynamic model of the large-bore engine was constructed. As shown in fig. 5, the engine has V-type structure with twelve cylinders and adopts supercharger and intercooler to improve the output power. The cylinder diameter and stroke were 190 millimeter and 210 millimeters, respectively. The rated power and speed for generate electric power were 680 kilowatt and 1000 rotation per minute, respectively. In order to calculate the heat transfer rate in cylinder, Woschnil 1978 model was adopted. The friction loss was confirmed by Chen-Flynn empirical formulas [10].

Fractal combustion model

As the injection law of fuel has influence on macroscopic charge motion and combustion in cylinder, fractal combustion model was used to calculate heat release [11,12].

$$\frac{dm_b}{dt} = \rho_u \times A_T \times S_L \tag{4}$$

Where dm_b/dt represents the burning rate of mixture, ρ_u is the density of the unburned mixture, S_L represents the laminar burning speed, A_T refers to the flame front area propagating within the turbulent flow field.

Influenced by the turbulence density of the in-cylinder charge, A_T has a relationship with laminar flame area and fluctuation factors.

$$A_T = \left(\frac{I_{max}}{I_{min}}\right)^{D_3-2} A_L \tag{5}$$

Where A_L is the laminar flame area, which is confirmed by geometric parameters of the cylinder; I_{min} and I_{max} are the minimum and maximum fluctuation factors related to Reynolds number, respectively. D_3 reflects the distortion of the flame, i.e. the fractal dimension of the flame.

Verification of the thermodynamic model

To verify the feasibility of thermodynamic model of the gaseous fuel engine, a large-bore engine prototype which is normally used for electricity generation in coal mine was developed. To improve the engine performance, a novel multi-point natural gas supply system was adopted instead of the continuous injection system. Before inputting the natural gas into the twelve injectors, the gas pressure was reduced by a relief valve. Mechanical energy output from the engine was transformed to electric energy by the electric generator. Host computer and DSP control system were used to control the twelve injection devices. Both the simulation model and the engine prototype adopted the same injection strategy without optimization.

As shown in fig. 6, under full load operations (from 700r/min to 1500r/min) and partial load operations (under the rated speed 1000r/min), the simulation and test results were in high degree of coincidence, with maximum error less than 6%, which indicates the feasibility of the thermodynamic model in optimization of engine performance.

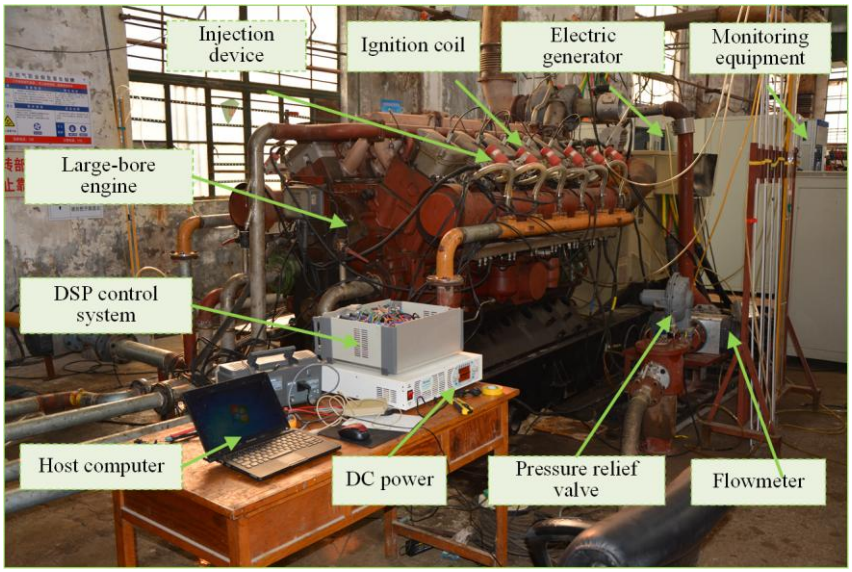

Fig. 5. Engine prototype with multi-point fuel supply system

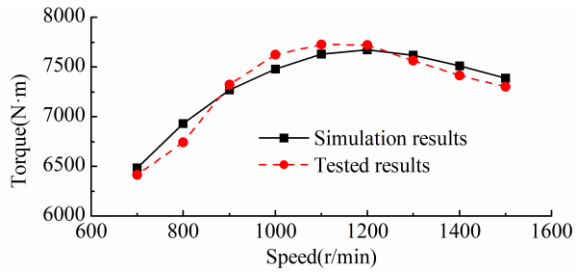

(a) Power verification under full load

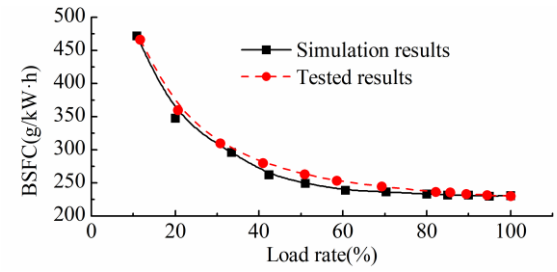

(b) Efficiency verification under rated speed

Fig. 6. Verification of the thermodynamic model

B. Development of injection rate model

Injection rate of the new-type device is a key factor influencing the precise control of cyclic fuel supply. As shown in fig.7, an experiment bench of the injector with large flow was developed. There are two factors influencing the injection rate: one is the pressure difference between the inlet and outlet of the device, and the other one is the valve lift. Consequently, two-factor orthogonal test was designed to confirm the injection flow function.

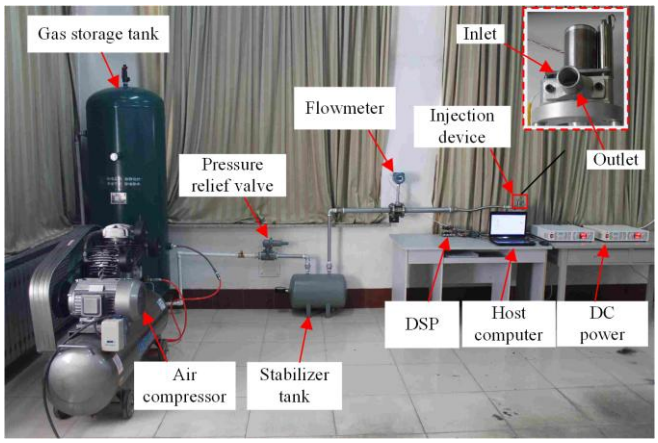

Fig. 7. The flow test of the injection device

According to the test results in fig. 8, the natural gas flow rate increased in proportion to the two factors. Under a given pressure difference, with the increase of valve lift, the influence of it on flow rate decreased. Based on the test data and using numerical fitting method, the two-factor flow function was created, as shown in equation 6. Numerical analysis results showed that the correlation coefficient was 0.99962 and the root mean square error was 0.54621. The fitting equation showed high precision in the calculation of cyclic natural gas injection.

$$r_m = \begin{bmatrix} -0.273 & -18.872 & 0.162 & 255.601 & 11.020 & -30.391 & 1.033 \end{bmatrix} \begin{bmatrix} l^3 \\ pl^3 \\ l^2 \\ pl \\ l \\ p \\ 1 \end{bmatrix} \quad (6)$$

Where r_m is the mass flow rate of natural gas, p is the pressure difference, and l is the lift.

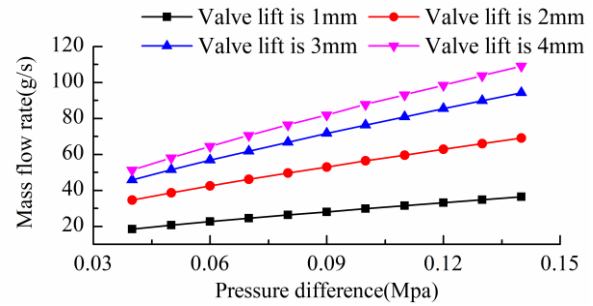

Fig. 8. Mass flow of the injection device

C. Development of optimization model

As shown in fig. 9, an optimization model was constructed based on the thermodynamic model and genetic algorithm (GA)[13]. For any given operation, the injection pulse width remained constant, but the starting and ending times of the injection were generated by the genetic algorithm randomly. According to the injection times from the GA module, the thermodynamic model showed a great performance in calculating the brake specific fuel consumption (BSFC) and presenting feedback for the GA module. Referring to the feedback BSFC, new population of injection times was obtained by variation and evolution. The optimization iteration did not stop until the optimal BSFC was achieved.

D. Optimization of injection strategy

Fig. 10 shows the optimal starting and ending times of the injection under various speed and load conditions, which are all expressed with corresponding crank angles to simplify control strategy. In general, as the effective injection pulse width decreased with the increase of engine speed, the starting time of injection (corresponding crank angles) advanced with the increase of engine speed. Engine speed had little influence on injection ending time. Under a given speed, a larger scavenging overlap angle was required for the higher load to reduce cylinder temperature and avoid detonation. Consequently, under high load conditions, a late injection is preferred to prevent the mixture from flowing into exhaust system within the scavenging overlap.

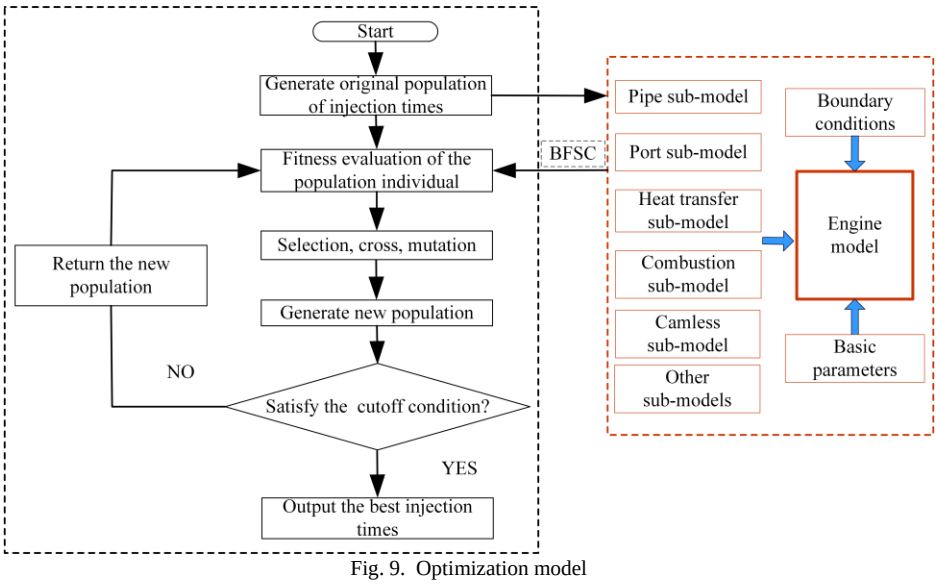

Fig. 9. Optimization model

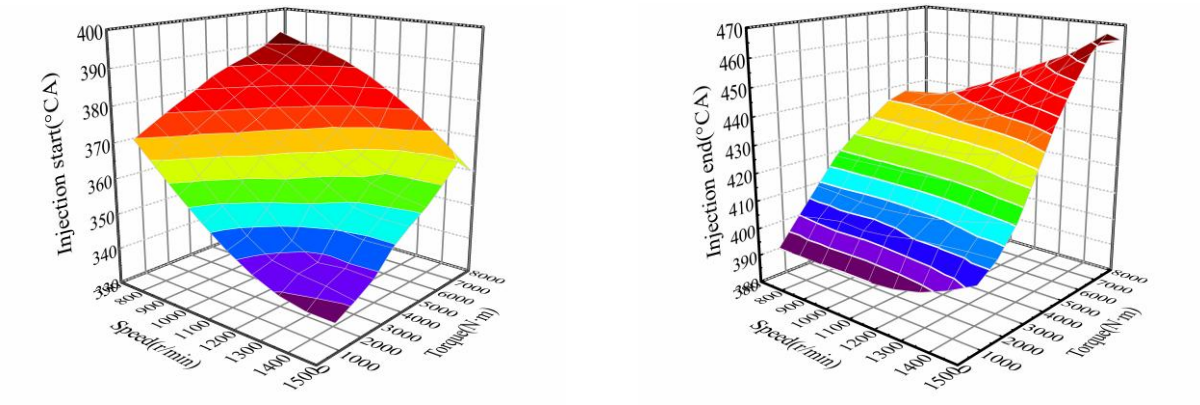

(a) The optimal injection start time (b) The optimal injection end time

Fig. 10. The optimal injection strategy

IV. Verification

A. Verification of efficiency

To compare the effect of fuel supply system on engine efficiency, cyclic fuel consumption of the original engine with the continuous fuel supply system and the proposed engine with multi-point gaseous fuel injection system were tested. As shown in fig. 11, the multi-point fuel injection system showed greater advantage in gaseous fuel consumption from static state of engine to rated condition.

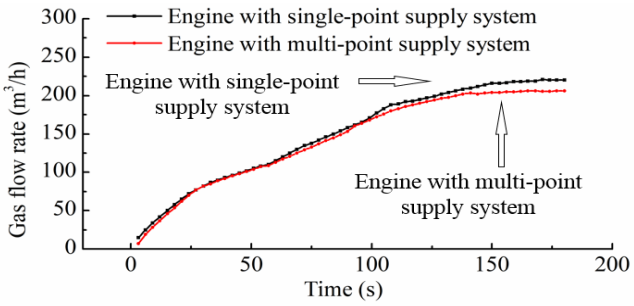

Fig. 11. Natural gas flow rate versus time curve

As shown in formula 7, in order to qualify the gaseous fuel efficiency of the engine, effective fuel consumption rate was defined as the gaseous fuel consumption per output energy from the engine.

$$b_e = \frac{m}{P} = \frac{\rho v}{pt} = \frac{\rho}{p} \cdot l \tag{7}$$

Where b_e is the effective fuel consumption rate defined to measure engine performance, m is the mass of gaseous fuel, P represents the output energy of engine, ρ is the gaseous fuel density under standard condition, p represents engine power, and l is the volume flow.

According to the optimized effective fuel consumption rate shown in fig. 12, the fuel efficiency of the engine was improved by 6.4% under full load and by 5.7% under the rated speed of 1000r/min.

B. Verification of cylinder uniformity

The cylinder uniformity has a significant influence on the large-bore engine. To verify the enhancing effect of the multi-point gas injection system on engine performance, the exhaust temperatures of the twelve cylinders were tested. The difference in exhaust temperature can be used to characterize the volatility of cylinder uniformity. Fig. 13 shows the temperatures of the first, sixth, ninth and twelfth cylinder under the given power generation condition. According to the test result, it can be confirmed that exhaust temperatures of the new engine with twelve injectors tended to be stable. Furthermore, due to the unstable combustion, the exhaust temperature of the original engine fluctuated much more significantly than that of the proposed engine.

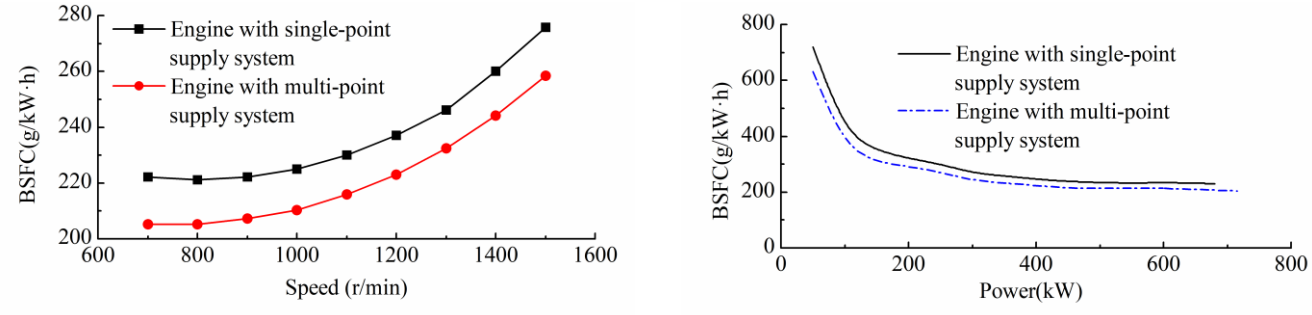

(a) BSFC under full load (b) BSFC under the rated speed

Fig. 12. Improvement of BSFC under full load and rated speed

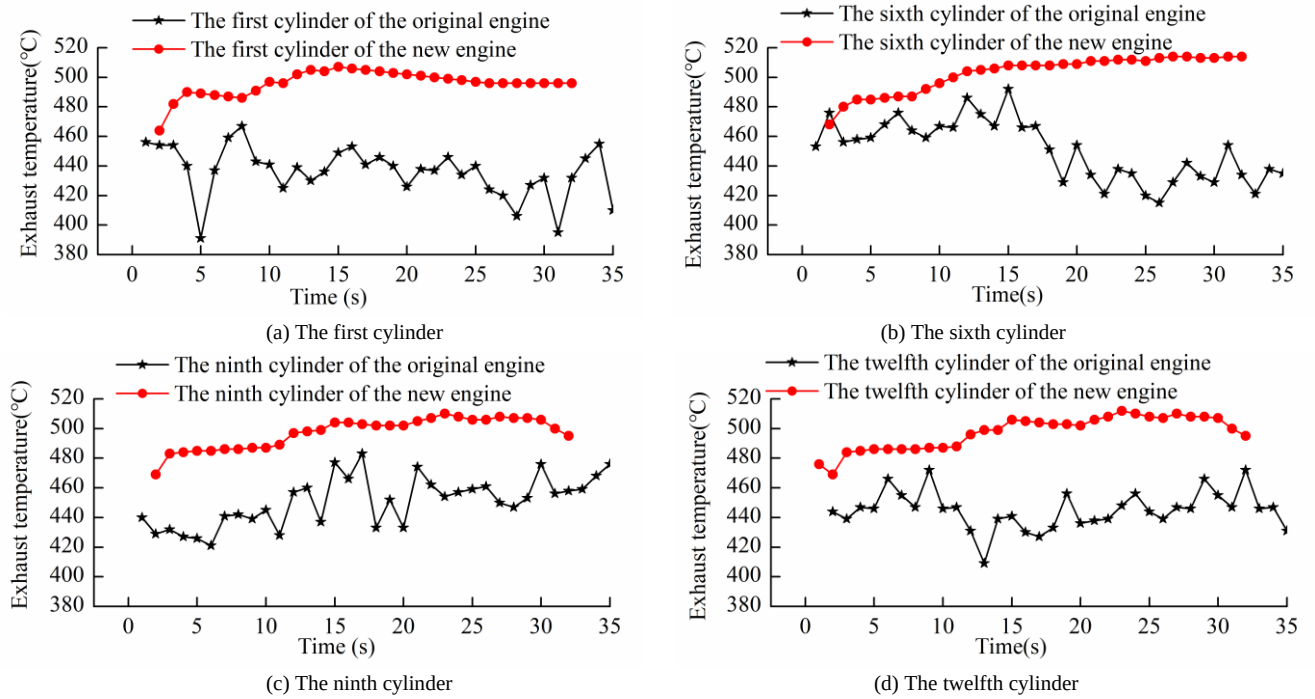

(a) The first cylinder

(b) The sixth cylinder

(c) The ninth cylinder

(d) The twelfth cylinder

Fig. 13. Exhaust temperature in four cylinders

To quantify the temperature fluctuation, function as follow was developed.

$$\begin{cases} \sigma(T)=\sqrt{\dfrac{1}{i-1}\sum_{i=1}^{i}(Ti-\overline{T})^2} \\ \overline{T}=\dfrac{1}{i}\sum_{i=1}^{i}T_i \end{cases} \tag{8}$$

Where T is the exhaust temperature, $\sigma(T)$ is the standard deviation, i is the cylinder number, and $\overline{T}$ is the average exhaust temperature.

As shown in fig.14, under the rated operation, the maximum $\sigma(T)$ of the proposed engine was 12.31℃, while that of the original engine was 20.15℃, showing a increasing rate of 63.69%. Moreover, each cylinder of the original engine showed a greater fluctuation of exhaust temperature than that of the proposed engine. The biggest difference of exhaust temperature was found in the first cylinders of the two engines, between which the deviation was 91.92%.

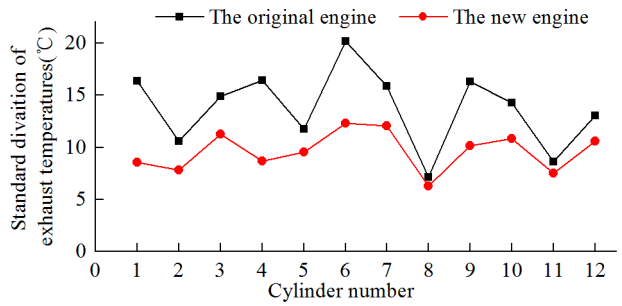

Fig. 14. Standard deviation of exhaust temperatures

The exhaust temperature fluctuation is proposed as follow to measure to the cylinder uniformity.

$$C_0V(T)=\sigma(T)/\overline{T}\times 100\% \tag{9}$$

As shown in fig. 15, under the rated operation, the biggest exhaust temperature fluctuation of the original engine was 6.64%, while that of the proposed engine was 3.37%. Moreover, the proposed engine showed better uniformity. The average exhaust temperature fluctuation of the proposed engine was 2.67%, which was lower than that of the original one by 37.47%.

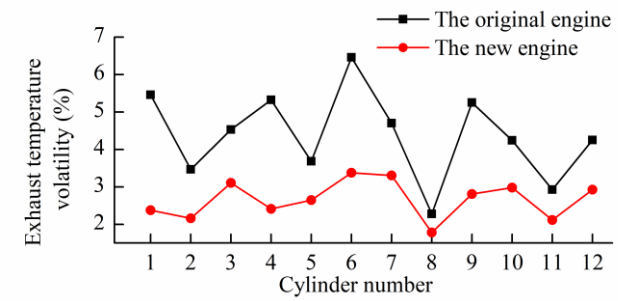

Fig. 15. Volatility of exhaust temperature

C. *Verification of power performance*

Two kinds of tests were conducted to verify the improvement of the engine power performance. As shown in Fig 16(a). due to the continuous fuel supply, natural gas existed in the intake manifolds of the original engine with single-point supply system. In order to avoid flash back in the intake manifolds, the natural gas was limited during the start-up process. Thanks to the real-time controllability of the multi-point supply system, the flash back was solved and consequently the start-up time was reduced by 21.3%.

The other test was about the external characteristics of the engine torque, as shown in Fig 16(b). As the cylinder uniformity was improved significantly, more natural gas was injected under the full load condition. The torque of proposed engine under full load was increased by 4.7% in comparison with that of the original engine.

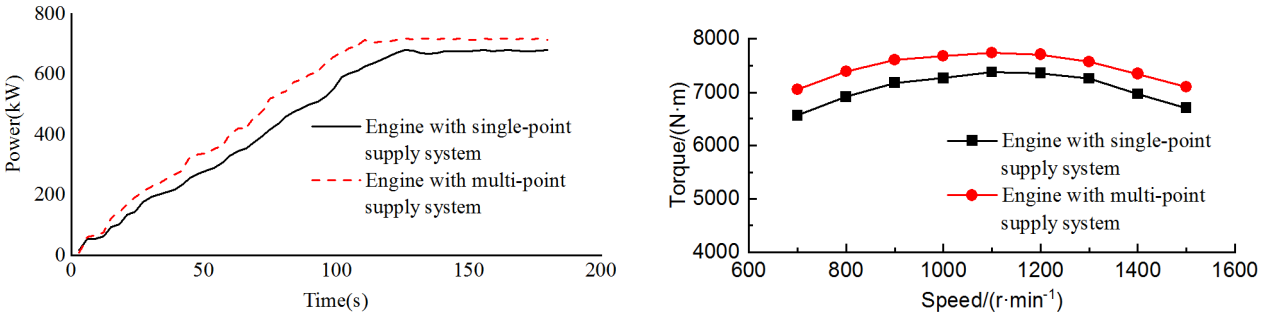

(a) Start-up performance

(b) External characteristics of torque

Fig. 16. Verification of power performance

V. Conclusion

In this paper, a multi-point natural gas injection system for large-bore engine was developed. The injection time of the system was optimized and verified based on thermodynamic model of the engine and genetic algorithm. For the large-bore natural gas engine, the injection device in discoid outlet structure can achieve cyclic fuel injection. With an inverse system control method, both high response speed and low seating velocity of the injection device were achieved. Typically, the valve closing process was completed within 5ms, and the seating velocity was about 3mm/s. The proposed engine with multi-point natural gas injection system had a better performance than the engine with continuous gas supply system. Compared to original engine, the fuel efficiency of the proposed engine was improved by 6.4% under full load and by 5.7% under the rated speed. The volatility of exhaust temperature in twelve cylinders was reduced by 37.47% under the rated working condition. Furthermore, the start-up time of proposed engine was reduced by 21.3% and the torque under full load was increased by 4.7%.

References

[1] J. Ren, Z.Y. Wang, H. Zhong, and et al, "Influence of performance characteristic of a gaseous fuel supply system on hydrocarbon emissions of a dual-fuel engine," *P. I. MECH. ENG. D-J. AUT.*, vol. 214, no.8, pp973-977, 2000.

[2] J. Czerwinski, P. Comte and Y., "Zimmerli. Investigations of the Gas Injection System on a HDCNG Engine," *SAE paper*: 2003-01-0625.

[3] H. Park, S. Lee, J. Jeong, and et al., "Design of the Compressor-Assisted LNG fuel gas supply system," *Energy*, vol. 158, no.1, pp1017-1027, 2018.

[4] Hyunjun P., Sanghuk L., Jinyeong J., and et al., "Design of the compressor-assisted LNG fuel gas supply system," *Energy*, vol.158, pp1017-1027, 2018.

[5] S. Li., "Study on Combustion System of the High Performance and Large Power Natural Gas Engine," M.S. thesis, Dept. Electron. Eng., Shandong Univ., Jinan, China, 2013.

[6] W. Ge, "Electronically Controlled Injection Device for Gaseous Fuel," Invention Patent of China, 20111033254.8, 2011.

[7] W. Ge, S. Chang, B. Sun, and et al., "Flow Characteristics of Electronically Controlled Gas Fuel Injection Device for Heavy-duty Engine," *Journal of Nanjing University of Science and Technology*, vol.36, no.4, pp669-673,2012.

[8] A. Boretti, P. Lappas, B. Zhang, and et al., "CNG Fueling Strategies for Commercial Vehicles Engines - a Literature Review," *SAE paper*: 2013-01-2812.

[9] F. Nicora, T. Santos and H. Rezende., "Natural Gas Refuse Collection Medium Truck, Driving Change in Brazil," *SAE paper*: 2013-36-0491.

[10] D. Jiang, *Principle of Higher Internal Combustion Engine*, Xi'an: Xi'an Jiao Tong University Press, 2002, chap 3.

[11] B. Sun, S. Chang and L. Liu, "A Research on Internal Exhaust Gas Recirculation by Using a Control Strategy of Intake Valve Secondary-opening," *Automotive Engineering*, vol.36, no.2, pp145-150, 2014.

[12] Tarek A. El-Mihoub, Adrian A. Hopgood, Lars Nolle, and et al., "Hybrid Genetic Algorithms: A Review," *Engineering Letters*, vol. 13, no.2, pp124-137, 2006.

[13] Krishna, B. Murali and J. M. Mallikarjuna., "Effect of Cavity in a Pentroof Piston on the Engine In-cylinder Tumble Flows - An Investigation by Particle Image Velocimetry," *Engineering Letters*, vol.17, no.3, pp195-199, 2009.